

CHAPTER 5

MECHANICAL PROPERTIES AND IRRADIATION CREEP OF GRAPHITE

B.T. Kelly and B.J. Marsden

In the unirradiated state orthodox polycrystalline graphites are near brittle materials with low elastic moduli ($\sim 10^{11}$ dyn.cm⁻²). The mechanical strengths and the elastic moduli decrease slowly with increasing heat treatment temperature and the stress-strain curves become increasingly non-linear. The strain to failure is roughly one order of magnitude greater in compression than tension.

Normal extruded or moulded polycrystalline graphite possesses an axis of symmetry parallel to the extrusion or pressing direction and thus has the same symmetry as a graphite crystal. The same symmetry applies to highly oriented pyrolytic graphite and thus in every case the elastic deformation can be described by five elastic compliances S_{ij} or moduli C_{ij} (the same symbols with a dash apply to crystal values). An isotropic graphite requires only three compliances or moduli. Table V.1 compares typical elastic compliances for an isotropic graphite (Gilsocarbon) and an anisotropic graphite (Pile Grade A) measured at small strains (Goggin and Reynolds, 1967).

TABLE V.1

TYPICAL ELASTIC COMPLIANCES FOR ANISOTROPIC AND ISOTROPIC GRAPHITE

Elastic Compliance	Pile Grade A (Anisotropic) cm ² /dyn	Gilsocarbon (Isotropic) cm ² /dyn
S_{11}	2.150×10^{-11}	1.370×10^{-11}
S_{12}	-0.127×10^{-11}	-0.148×10^{-11}
S_{13}	-0.123×10^{-11}	-
S_{33}	1.087×10^{-11}	-
S_{44}	3.333×10^{-11}	3.030×10^{-11}

The elastic constants reported in the literature are generally determined in one of two ways: dynamically, that is at very small strains (although not generally well defined); or quasi-statically where the strain is measured as a function of stress. The non-linearity of the stress-strain curves presents a difficulty since the compliances increase with strain, there is significant hysteresis on unloading and a permanent set occurs. Fig 5.1 shows the stress-strain relations of an unirradiated polycrystalline graphite.

The effect of irradiation with fast neutrons is to initially increase the elastic moduli by substantial factors, depending upon the material, at low doses, followed by subsequent increases and decreases. The effects of irradiation on the crystal elastic constants have been examined using the best available single crystals (Ticonderoga flake) or highly oriented pyrolytic graphite. Very thorough studies of this type were reported by Seldin and Nezbeda (1970). Highly oriented pyrolytic graphite and carefully chosen Ticonderoga flakes were irradiated at 50, 650 and 1000 °C. It was found that in each case only the crystal elastic constants C_{33} and C_{44} changed. At 50 °C the elastic modulus C_{33} in highly oriented pyrolytic graphite decreased slightly from an initial value of 3.65×10^{11} dyn.cm⁻², the expected value for

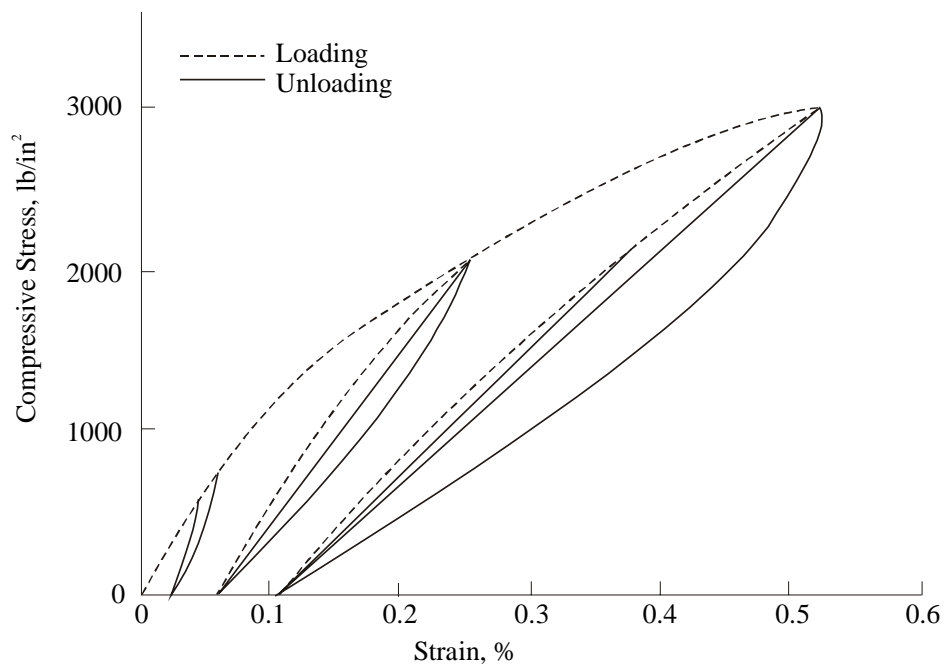
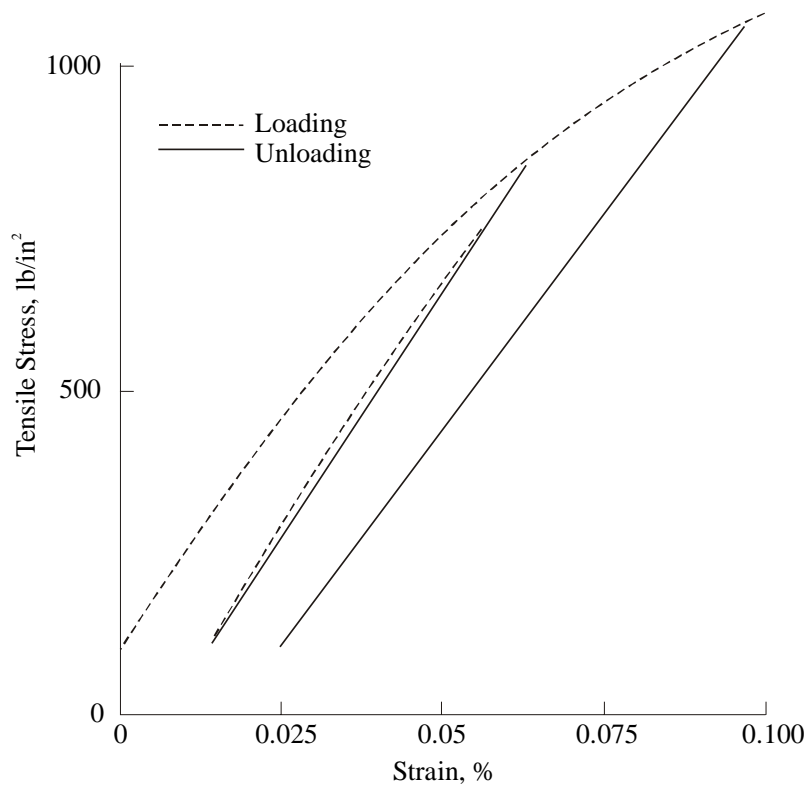


Figure 5.1 Stress and strain diagrams for unirradiated graphite

the crystal in that direction. The dose range examined was $\sim 10^{19}$ n.cm⁻². The changes in C_{44} were much larger, from initial values of 0.021 - 0.030 x 10¹¹ dyn.cm⁻² to a near saturation value of 0.4 x 10¹¹ dyn.cm⁻², close to the value expected for a perfect crystal. The single crystal samples irradiated at 650 and 1000 °C showed large increases in C_{44} also, tending to values of ~ 0.3 x 10¹¹ dyn.cm⁻², but only very small changes were observed in the C_{44} of the pyrolytic graphite.

Baker and Kelly (1964) reported increases in the C_{44} of single crystal graphite on neutron irradiation at ~ 100 °C by an order of magnitude. Jenkins and Jouquet (1968) obtained large increases in C_{44} in hot-worked pyrolytic graphite on irradiation at 30 °C. Summers *et al* (1966) reported decreases in C_{33} in highly oriented pyrolytic graphite following irradiation at 150 °C.

Ayasse and Bonjour (1976) irradiated highly oriented pyrolytic graphite at 77 K and measured the changes in C_{33} . The initial value was found to be 3.4 x 10¹¹ dyn.cm⁻². C_{33} was decreased with increasing dose, by about 7% at a dose of 4 x 10¹⁸ n.cm⁻² ($E > 1$ MeV). The recovery of these changes with annealing was gradual, rather similar to dimensional changes perpendicular to the deposition plane (about 1.5% at peak dose).

The elastic moduli C_{33} and C_{44} are both associated with the interlayer forces, which might be expected to weaken as the interlayer spacing increased with the introduction of lattice defects. The reduction in C_{33} with dose is readily explained in this way, but the large and material dependent changes in C_{44} have been attributed to the pinning of glissile dislocations in the basal planes, which normally decrease the shear constants. It is known that in very pure metals such as copper the elastic moduli are reduced by 5-10% because of the presence of glissile dislocations which respond to shear stresses. The graphite crystal is unusual in having only two slip systems in the basal planes and the near two-dimensional nature of the crystal probably removes obstacles to dislocation movement in basal plane shear.

It is fortunate that very thorough transmission electron microscope studies on crystalline graphite (Amelinckx and Delavignette, 1960; Amelinckx *et al*, 1966) have permitted detailed study of the basal dislocations. The effect of the basal dislocations is to reduce the crystal shear modulus C_{44} . The basal dislocations are split into partial dislocations with Burger's vector $1/3a$ ($10\bar{1}0$). The total Burger's vector of the two partials, which constitute the total dislocation, is

$$\frac{1}{3}a(2\bar{1}\bar{1}0) = \frac{1}{3}a(10\bar{1}0) + \frac{1}{3}a(1\bar{1}00) \quad (5.1)$$

In isolated full dislocations the separation of the partial dislocations varies from ~ 500 x 10⁻⁸ cm to 1000 x 10⁻⁸ cm depending upon the orientation in the basal planes.

The basal dislocations are readily observed as isolated dislocations or as triangular networks which are 50% stacking faults with ABC stacking. The large separation of the dislocations compared to the crystallite size in the basal planes in polycrystalline graphites means that the dislocation distribution is more likely to consist of the triangular networks which may be responsible for the roughly one layer in six which is apparently mis-stacked in well crystallised polycrystalline graphite, although such a correspondence has not been directly established.

The theory of the effect of isolated dislocations on the elastic moduli has been considered by many workers, particularly Eshelby (1949), Friedel (1953) and Mott (1952). Assume that a crystal contains a uniform density Λ_0 of dislocations in the basal planes and further suppose that under an applied shear stress τ the dislocations glide an average distance x in the direction of the

stress. This adds a strain

$$\varepsilon_p = \Lambda_0 \mathbf{b} x \quad (5.2)$$

to the elastic strain τ/C_{44} , where \mathbf{b} is the Burger's vector. Two quite distinct models have been formulated to estimate the value of x for graphite.

Friedel (1953) described a model in which the isolated dislocations are in the form of N_0 independent arcs per unit volume, each of length L_0 . Equation (5.2) can then be written

$$\varepsilon_p = N_0 \mathbf{b} \alpha \quad (5.3)$$

where α is the area swept out by each arc due to the stress τ . If the line tension of the dislocation is T , Friedel showed that

$$\alpha = \frac{L_0^3 \mathbf{b} \tau}{12T} \quad (5.4)$$

which leads to an apparent decrease in the shear modulus $G (=C_{44})$ for the crystal of

$$\frac{\Delta G}{G} = \frac{G \mathbf{b}^2 N_0 L_0^3}{12T} \quad (5.5)$$

Chou and Eshelby (1962) presented calculations of the line tension T for both edge and screw dislocations.

Woolley (1965) formulated a model in which the dislocations react to form twist boundaries perpendicular to the crystal hexagonal axis. It is supposed that these twist boundaries are separated by a distance H and confined to slip planes of diameter L_a . The whole boundary now moves under the shear stress τ . Woolley considered the behaviour of a set of n parallel dislocations of which the outer pair, at $\pm L_a$, were firmly fixed and obtained for large n

$$x = \frac{\pi L_a^2 \tau}{K_s b n} \quad (5.6)$$

where K_s is a mean elastic modulus (Eshelby, 1949).

In each case the apparent crystal shear modulus is given by

$$C_{44}^1 = \frac{C_{44}}{1+B} \quad (5.7)$$

where B is the effect of the glissile basal dislocations. Equations (5.5) and (5.7) can give large reductions in C_{44} using reasonable values for the parameters.

It would be expected from this model that the apparent mechanical shear modulus of graphite crystallites would vary from material to material, but if the dislocations can be pinned by irradiation and their strain contribution removed then the shear moduli should all tend to the same value.

Kelly (1964) applied equation (5.5) to the changes in Young's modulus with dose in polycrystalline graphite, finding that if pinning points on dislocation lines changed the arc lengths L , and number of arcs N , in accordance with

$$\Lambda_0 = N_0 L_0 = N L \quad (5.8)$$

and assumed linear increase of pinning points with dose, then the data due to Simmons (1957) could be fitted with $B = 2$. This analysis is only valid if, for small doses, the elastic moduli of the polycrystalline graphite are proportional to the crystal shear constant C_{44} . Consideration of the elastic energy of a porous polycrystal shows that this is likely to be true, particularly if there is a tendency for the uniform stress approximation to be appropriate (Kelly, 1964).

Measurements of modulus changes at higher doses were made following irradiation at temperatures from 150 - 650 °C (Kelly, 1964) on Pile Grade A graphite. These results show that the fractional changes in Young's modulus are independent of direction, as expected if the macroscopic deformation is controlled by a single microscopic deformation model (basal shear). The results show two clearly different regions of behaviour. In irradiations below ~300 °C the Young's modulus increases by a factor of about 3, peaks and then decreases, followed by an increase and later still a catastrophic decrease followed by disintegration. In irradiations above 300 °C an initial increase occurs to a level which decreases with increasing temperature, remains constant, then increases and finally falls. In both regions increasing the irradiation temperature increases the dose at which any characteristic feature of the changes occurs.

Data on other graphites are not so extensive. Results on Gilsocarbon graphite have been presented by Birch (1981), and Goggin and Reynolds (1967), for experiments carried out at ambient. Birch also studied the changes in the stress-strain curves, while both studies measured the changes in the shear modulus and Poisson's ratio. Taylor *et al* (1967) measured the changes in elastic modulus and Poisson's ratio of three isotropic graphites following irradiation at 150 °C. The pattern of the data is similar to that observed in Pile Grade A graphite, but there are significant differences in the data of Birch, and Goggin and Reynolds, in the shear modulus behaviour. The changes in the shear modulus at small strains measured by Goggin and Reynolds are the same as those of the Young's modulus, but in the study by Birch the changes are smaller. Goggin and Reynolds measured the changes in the elastic constants at finite strains and found that they differed quite significantly from those at small strains (in some cases quite significantly), this has not been explained. The relationship

$$G = \frac{E}{2(1 + \nu)} \quad (5.9)$$

where G is the shear modulus, E is the Young's modulus and ν is the Poisson's ratio may be derived assuming only isotropy and the principle of superposition. Goggin and Reynolds (1967) measured E , G and ν on isotropic graphite before and after irradiation. They found

$$G = 3.3 \times 10^{10} \text{ dyn.cm}^{-2} \quad \frac{E}{2(1 + \nu)} = 3.28 \times 10^{10} \text{ dyn.cm}^{-2}$$

before irradiation and

$$G = 11 \times 10^{10} \text{ dyn.cm}^{-2} \quad \frac{E}{2(1+\nu)} = 12.4 \times 10^{10} \text{ dyn.cm}^{-2}$$

following a brief irradiation at ambient temperature. The agreement with theory suggests that these data are correct with regard to the shear modulus changes.

Extensive data have recently become available on the Young's modulus, shear modulus and Poisson's ratio changes in the near isotropic H-451 nuclear graphite. Equation (5.9) is quite well obeyed (the deviation from isotropy may have some effect) in irradiations at temperatures from 600 - 1200 °C, even when pore generation is present.

The following explanation of these results has been proposed. Simmons (1957) and Kelly (1964) proposed that all of the elastic compliances of porous polycrystalline graphite are dominated by the basal shear of the component crystallites. This assumption is expressed as

$$\begin{aligned} S_{ij} &= \alpha_{ij} S_{44}^1 \\ C_{ij} &= \beta_{ij} C_{44}^1 \end{aligned} \quad (5.10)$$

where $C_{44}^1 = 1/S_{44}^1$ and α_{ij} and β_{ij} are "structure factors". If this is correct it also explains the following:

- (i) The similarity of all of the stress-strain relationships of a polycrystalline graphite, all of which exhibit non-linearity, permanent set and hysteresis.
- (ii) In irradiations to small doses all of the elastic compliances and moduli change by the same factor. Only the shear constant S_{44}^1 is significantly increased in single crystals and highly oriented pyrolytic graphite.

Equation (5.10) can be derived, either by assuming, as must be the case, that all of the elastic constants (compliances and moduli) must be linear functions of the five elastic compliances or moduli and noting the large difference in the shear constant term, or by equating the macroscopic strain energy of a graphite cube to the sum of the strain energies of the component crystallites. The likely dominance of shear strain energy leading to (5.10) is obvious. However equation (5.10) can only hold in a porous polycrystalline graphite, not in a fully dense material. This may be shown as follows.

In an isotropic body it is readily shown using the principle of superposition that

$$\text{Shear Modulus } G = \frac{E}{2(1+\nu)} \quad \text{Bulk Modulus } K = \frac{E}{3(1-2\nu)} \quad (5.11)$$

Markham (1962) calculated the elastic constants of solid isotropic graphite and obtained, neglecting all terms except those which represent basal shear

$$S_{11}^1 = \frac{1}{E} = \frac{2}{15} S_{44}^1 \quad S_{12}^1 = -\frac{1}{15} S_{44}^1 \quad S_{44}^1 = \frac{1}{G} = \frac{6}{15} S_{44}^1 \quad (5.12)$$

which leads in the conventional units to

$$\frac{E}{G} = 3 \quad \nu = \frac{1}{2} \quad (5.13)$$

which do not compare favourably with the observed values $E/G = 2.5$, $\nu = 0.2$, and also predicts $K = \infty$. The same conclusion may be obtained for the compressibility of anisotropic graphite without porosity, so that the presence of porosity is essential to equation (5.10).

In irradiations below ~ 300 °C the initial rise in modulus is followed by a decrease of similar magnitude. Kelly (1964) postulated that this was a decrease in the shear constant C_{44} as the pinning fields of point defects overlapped and allowed the dislocation strain to be re-established, but Woolley (1965) suggested that it was due to the lattice distortion caused by point defects at these temperatures which reduced the lattice shear constant. The fall in C_{33} observed by Summers *et al* (1966) in irradiations of highly oriented pyrolytic graphite at 150 °C supports this explanation because the glissile dislocations have no effect on C_{33} (or only a small effect due to misorientation). The lattice changes are much smaller for irradiations above 300 °C and the changes in the interlayer spacing are too small to reduce C_{44} and C_{33} and so the decrease does not occur. In both cases this stage of reflecting changes in the crystal elastic constants C_{44} rather than changes in the α_{ij} or β_{ij} is succeeded by a dose range where the opposite occurs and the crystallite dimensional changes modify the porosity and produce both increases and decreases in the α and β factors. The first change is an increase in β_{ij} (decrease in α_{ij}) due to a decrease in porosity, followed by a decrease in β_{ij} due to the generation of new pore space. These changes have been analysed by Kelly and Burchell (1994a) and shown to be a unique function of X_T for a given graphite (X_T is defined in equation (5.21)). The final fall in β_{ij} signals disintegration of the polycrystalline graphite into roughly coke particle sized pieces.

The situation regarding the dose dependence of Poisson's ratio is unsatisfactory. At small doses where equation (5.10) applies without changes in α_{ij} or β_{ij} , it would be expected that Poisson's ratio(s) would remain constant since the C_{44}^1 cancels in Poisson's ratio which depends, in the shear-dominated model, only on ratios of α_{ij} 's. This is supported up to a point by experiment (Goggin and Reynolds, 1967).

There are no adequate data when the changes in α_{ij} or β_{ij} become significant - it is not obvious that these should change in the same ratio independent of α_{ij} , and thus changes in the Poisson's ratio may occur.

The effect of final heat treatment temperature on the initial modulus change at ambient temperature was first reported by Losty and Orchard (1963). It was found that the non-linearity of stress-strain curves, the permanent set and the increases in Young's modulus on irradiation increased with heat treatment temperature, becoming significant at about 1600 °C. The crystal lattice is essentially turbostratic for lower heat treatment temperatures leading to problems with the definition of a basal dislocation. As the lattice becomes more three dimensional, glissile dislocations can be defined and are created, thus giving rise to the reduction in the lattice shear constant. The presence of these dislocations leads to the proposed effects.

Brocklehurst and Kelly (1993) examined the effect of irradiation on a heat treated series of Pile Grade A graphite stock irradiated at 600 °C. The initial increases were smaller the lower the final heat treatment temperature, but otherwise there are the expected behaviour (a period where the modulus change is constant, followed by the structure dependent rise and fall). There is some indication in this work of a change in anisotropy with dose.

It was observed by Kinchin (1956) that if a graphite sample was mechanically distorted before irradiation and then irradiated in the distorted state at ambient temperature that the sample remained distorted post-irradiation when the mechanical restraint was removed. Perks and Simmons (1964) showed that samples irradiated under stress showed different dimensional changes to those irradiated unstressed. The effects were very small (~100 ppm), but were interpreted as showing that graphite showed creep under irradiation at temperatures where no thermal creep was observed.

Detailed studies of dimensional changes under stress have since been described by many authors including Davidson and Losty (1958), Losty (1960,1962) and Losty *et al* (1962). These authors used springs under dead weight load which showed strain and which did not require any correction for dimensional changes. Exposure of samples of this type in the Calder Hall reactors in the United Kingdom showed that after a short transient period the rate of spring extension was proportional to the applied stress and atomic displacement rate. The strain was apparently independent of irradiation temperature between 140 °C and 324 °C.

Experiments were carried out in compression at low doses by Losty *et al* (1962) using the Herald reactor with an irradiation temperature of 70 °C. Similar creep behaviour was observed. Perks and Simmons (1964) carried out experiments with graphite in tension using the PLUTO reactor. Creep strains were observed which were several times the elastic strain. The creep ratios referred to unit stress and dose were larger in the direction perpendicular to extrusion in an anisotropic graphite than parallel to it.

Morgan (1963) carried out experiments at 625 °C under compression. There were difficulties in separating the effects of stress level but the creep rates obtained were comparable with the other work.

Gray (1973) reported creep data on several graphites under compressive stress set at three different levels at temperatures of 550 and 800 °C. The measurements included thermal expansion coefficient measured parallel to the stress direction. The results were the first to show creep strains, which were less than linear with dose and apparently in some cases negative. (The creep strains were defined, as usual, as the difference in dimensions between a stressed sample and an unstressed control sample.) It was also clear that the thermal expansion coefficients in the stress direction were increased by the creep strain, although the changes varied with the graphite. The dimensional changes perpendicular to the stress were measured and the lateral strain ratios determined. The results were interpreted as showing that creep strain modified the dimensional change term so that the definition of creep is no longer correct (leading to the apparent negative creep strains). The lateral strain ratios varied from 0.5 (constant volume) to 0.3. The implications of this work were neglected for some years.

Kelly and Brocklehurst (1977) summarised creep studies carried out in the United Kingdom since 1964, including data taken in tension, compression and shear on a wide variety of graphites (including radiolytically pre-oxidised, and pre-irradiated without stress to high doses) exposed at temperatures from 140 - 1040 °C. The results of this work were summarised in the following equation, valid for 140 - 650 °C:

$$e_c = 0.23 \times 10^{-20} \frac{T}{E_0} \gamma + \frac{T}{E_0} \left(1 - \exp[-4 \times 10^{-20} \gamma] \right) \quad (5.14)$$

where e_c is the creep strain, T is the stress, γ is the dose (n.cm⁻² EDN) and E_0 is the static

Young's modulus prior to irradiation. The first term is the secondary creep strain, and the second the transient creep. It should be noted that both terms are inversely proportional to the unirradiated Young's modulus and the second term has the magnitude of one elastic strain. In the same work the lateral strain ratio was

$$e_c^l = 0.3e_c \quad (5.15)$$

slightly larger than the unirradiated Poisson's ratio of most of the graphites studied. The creep rate increases slowly at higher temperatures and this is allowed for by introduction of a temperature factor $\beta(T)$, which is unity at 650 °C and lower temperatures. This study included measurements of lateral strain due to creep (the creep Poisson's ratio), changes in thermal expansion coefficient, and recovery of creep strain both thermally and under irradiation without stress. Creep rate was also measured on graphite doped with ^{11}B to enhance the crystal dimensional change rate. The creep Poisson's ratio in this series of experiments was ~ 0.3 .

Irradiation creep experiments carried out by Kennedy and co-workers (1977, 1979) at 600 and 900 °C indicate that in addition to the change in the thermal expansion coefficient there is a small change in modulus. This is accompanied by a large change in Poisson's ratio, at 900 °C falling from a value of ~ 0.14 to zero at $\sim 2.5\%$ creep strain in H-451 graphite. This is at odds with the finding in the UK.

It is clear that the transient stress was recoverable in the presence of thermal or irradiation annealing in the absence of stress which indicates that it is associated with stored elastic energy.

For temperatures greater than ~ 300 °C the data from all sources agree that the creep rate is constant to ~ 650 °C and then gradually increases up to ~ 1400 °C and probably beyond. However at temperatures of 300 °C and below, data obtained by Kennedy (1966a, 1966b) and Platonov (1966) show an increase in creep rate with decreasing temperature. This disagrees with the studies carried out in the UK, Kelly and Brocklehurst (1977), which show the same creep rate in the range 140-330 °C as in the range 300-750 °C. This discrepancy has never been fully resolved. See Figs 5.2 (a), (b).

Two theories of irradiation creep have been proposed. In the first (Kelly and Foreman, 1974) is an irradiation creep model due to Cottrell in which the internal stress generated by the incompatibility of the crystal dimensional changes eventually brings the crystallites to yield point and allows the polycrystalline graphite to flow under external stress. The second model is the dislocation pinning-unpinning model. In unirradiated graphite, it is assumed that a high density of dislocations within the basal planes constrains deformation of the crystallite by a small concentration of pinning points. When the graphite is irradiated these dislocations may be pinned, depending on the dose and temperature, which leads to the increase in modulus. As these small clusters of 4 ± 2 atoms are short lived due to irradiation annealing there is only a temporary barrier to dislocation movement. Thus the pinning and unpinning of these dislocations due to irradiation will allow the crystal to flow in basal slip at a rate determined by the displacement of atoms.

To explain the pinning-unpinning theory of irradiation creep in graphite, Kelly and Brocklehurst (1972) considered the work done due to a stress T_{xx} at the macroscopic level on a volume of graphite divided into small volumes of graphite a at the microscopic level in unstressed and stressed graphite. They showed that the theoretical creep rate can be given by the difference between the strain rate in the unstressed graphite compared with that in the stressed graphite which leads to:

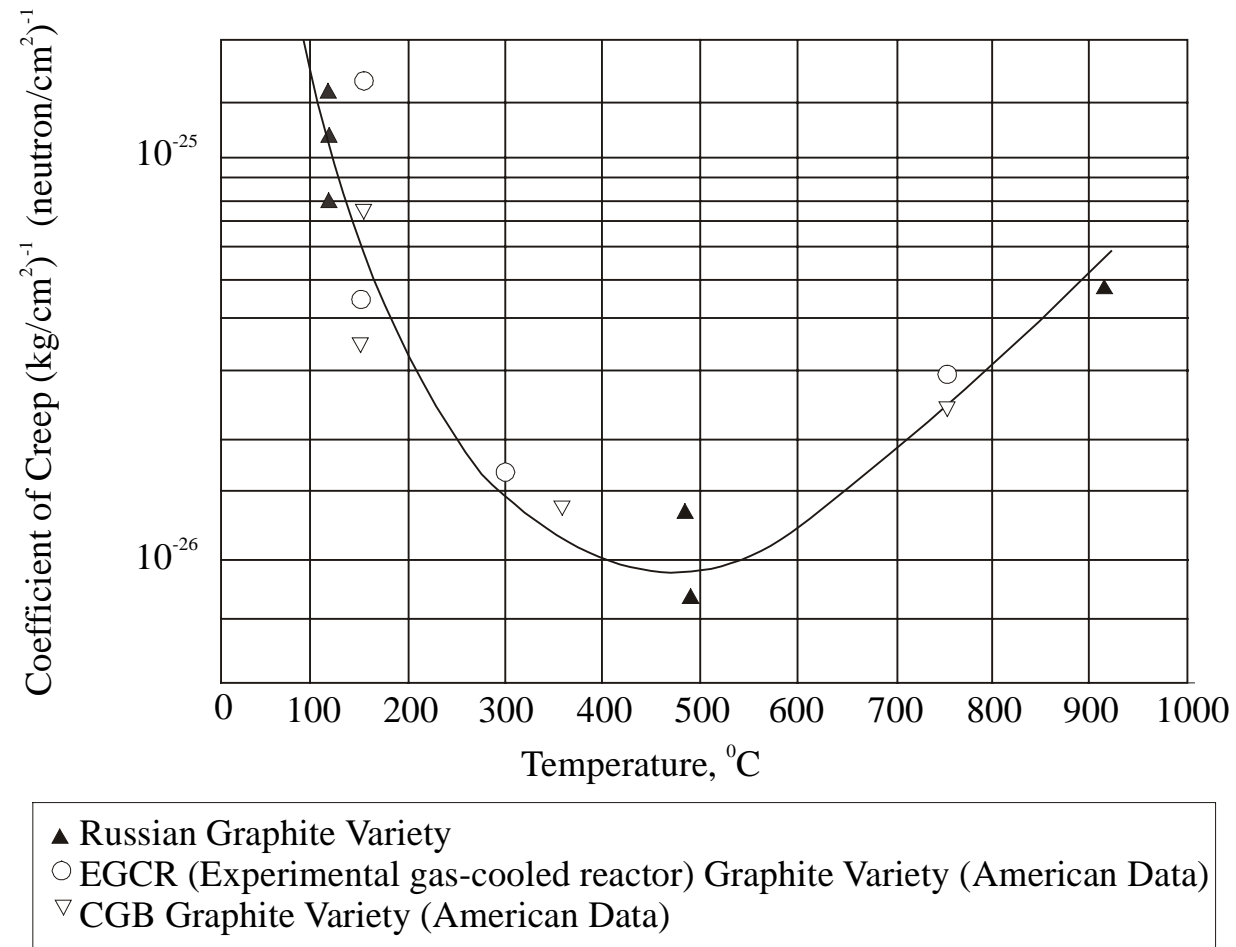


Figure 5.2 (a) Variation of creep rate with temperature: Russian and American data

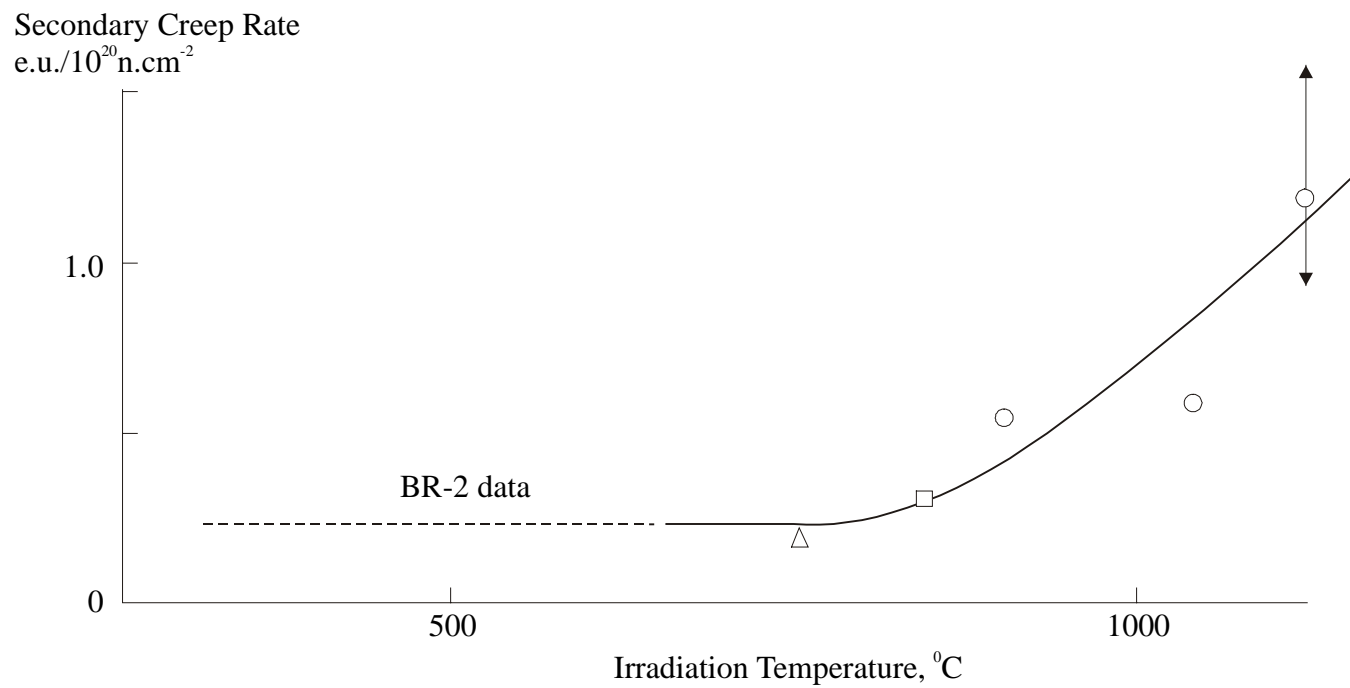


Figure 5.2(b) Variation of creep rate with temperature: UK data PLUTO

$$\dot{\epsilon}_c = \sum_r a_r \left| \frac{\partial[\sigma_{xz}]_r}{\partial T_{xx}} \Delta \dot{\epsilon}_{xzt} + \frac{\partial[\sigma_{yz}]_r}{\partial T_{xx}} \Delta \dot{\epsilon}_{yzt} + \frac{\partial[\sigma_{xy}]_r}{\partial T_{xx}} \Delta \dot{\epsilon}_{xyt} \right| \quad (5.16)$$

where $[\sigma_{ij}]_r$ denotes the stress on the r 'th volume of graphite in the crystal local co-ordinate system and

$$\Delta \dot{\epsilon}_{ijr} = [\dot{\epsilon}_{ij}]_r - [\dot{\epsilon}'_{ij}]_r \quad (5.17)$$

that is the difference in strain rate between the stressed and unstressed graphite, which by definition represents the creep strain rate.

Thus it is demonstrated that the dilation modes do not play a part, and the creep rate is determined by the crystal shear modes.

Making the assumptions that:

- (i) The only mode of crystal deformation is basal slip,
- (ii) The crystal strain rate for the graphite crystal in shear may be written as:

$$\Delta \dot{\epsilon}_{xzt} = K \left| \frac{\partial[\sigma_{xz}]_r}{\partial T_{xx}} \right| T_{xx} \quad (5.18)$$

$$\Delta \dot{\epsilon}_{yzt} = K \left[\frac{\partial[\sigma_{yz}]_r}{\partial T_{xx}} \right] T_{xx}$$

- (iii) and the S_{44} , ($C_{44} = S_{44}^{-1}$), compliance of the graphite crystal is much larger than the other crystal compliances,

leads to

$$\text{Creep rate} = KT_{xx} \frac{C_{44}}{E_{xx}} \quad (5.19)$$

Thus the creep rate is proportional to the reciprocal of the unirradiated graphite modulus measured in the direction of creep. This theory assumes that Poisson's ratio in creep is the same as the elastic Poisson's ratio, and as previously discussed, there are conflicting views on this. Fig 5.3 shows the mean ratio of total creep strains parallel and perpendicular to the loading direction measured on three different graphites as a function of differential change in length. This gives a Poisson's ratio in creep of ~ 0.3 compared with ~ 0.2 for the elastic case, although there is a substantial amount of scatter (due to the difficulty in measuring lateral strains on the specimens used) and the ratio is the same order as that of the elastic ratio.

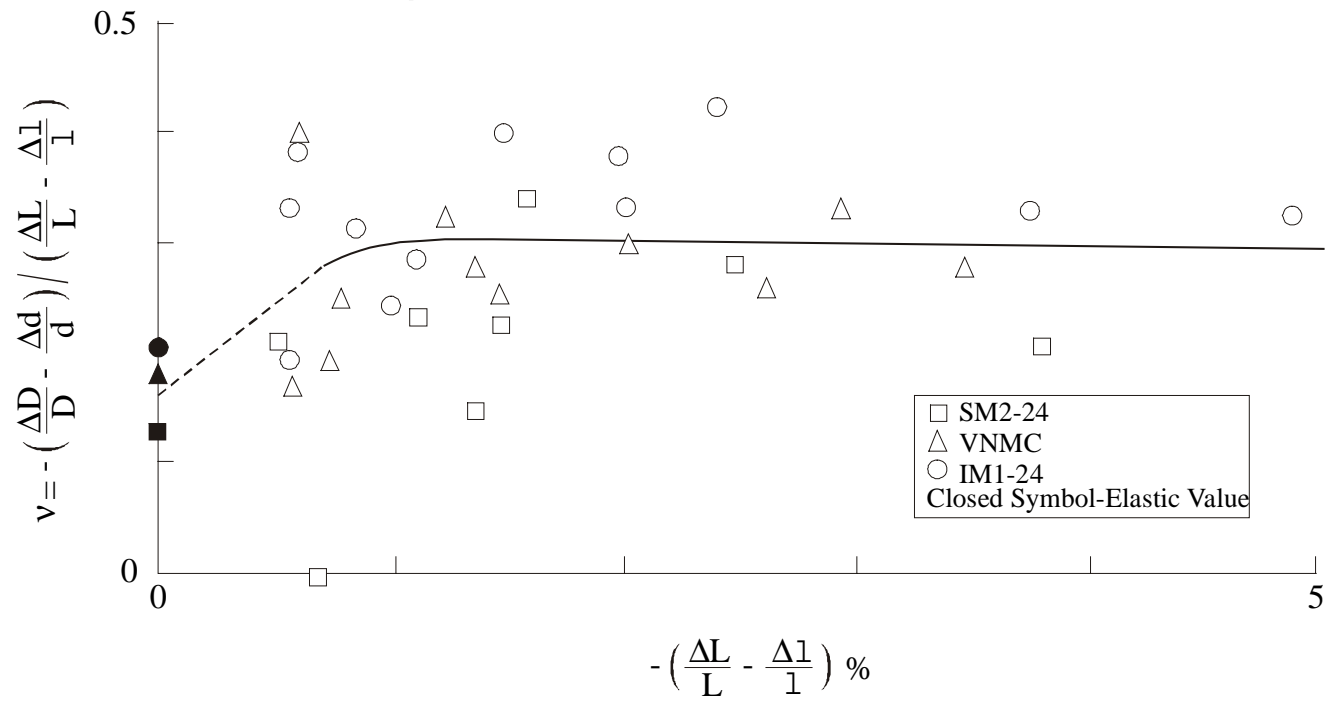


Figure 5.3 Creep Poisson's ratio as a function of longitudinal creep strain

More evidence for the pinning-unpinning model was given by experiments carried out on graphite doped with boron (¹¹B), Kelly and Brocklehurst (1977), to accelerate the irradiation damage to the crystallite. These experiments showed that the creep rate was not affected by the doping, indicating that the process of irradiation creep is displacement driven not damage driven, which collaborates in with the basal slip theory.

Early irradiation creep experiments had shown that changes to the thermal expansion coefficient in irradiated specimens appeared to be dependent on the level of creep strain. Those specimens with a significant amount of compressive creep strain had a higher coefficient measured in the direction of stress compared with the unstressed specimens, whereas specimens with significant tensile creep strain had a lower thermal expansion coefficient compared to the unstressed specimens, see Fig 5.4. This implies that creep strain modifies the dimensional change rate in the specimens, although annealing was shown to restore the thermal expansion coefficient to its original value but did not completely restore the creep deformation (Kelly and Brocklehurst, 1977). This finding also has implications related to dimensional change through the equation developed by Simmons (1965) discussed in Chapter 3.

To assess the interaction between creep strain, the thermal expansion coefficient and dimensional change rate, Kelly and Burchell (1994b) reanalysed the creep strain data for H-451 graphite using the Simmons (1965) theory for the relationship between the thermal expansion coefficient and dimensional change rate, giving

$$g_x = \left| \frac{\alpha_x - \alpha_a}{\alpha_c - \alpha_a} \right| \left(\frac{dX_T}{d\gamma} \right) + \frac{1}{X_a} \frac{dX_a}{d\gamma} \quad (5.20)$$

where α_x , α_a and α_c are the thermal expansion coefficients in the polycrystalline x direction and in the a and c crystallite axes. $(1/X_c)(dX_c/d\gamma)$ and $(1/X_a)(dX_a/d\gamma)$ are the crystal dimensional change rates and the shape factor is defined as:

$$\frac{dX_T}{d\gamma} = \frac{1}{X_c} \frac{dX_c}{d\gamma} - \frac{1}{X_a} \frac{dX_a}{d\gamma} \quad (5.21)$$

When graphite creeps under stress the thermal expansion coefficient increases with compressive creep strain and decreases with tensile creep strain, thus changing the dimensional change rate as given below:

$$g'_x = \left(\frac{\alpha'_x - \alpha_a}{\alpha_c - \alpha_a} \right) \left(\frac{dX_T}{d\gamma} \right) + \frac{1}{X_a} \frac{dX_a}{d\gamma} \quad (5.22)$$

The dash represents the change in the crept specimen. This leads to an apparent creep rate of

$$\frac{de'_c}{d\gamma} = \frac{de_c}{d\gamma} - \left| \frac{\alpha'_x - \alpha_x}{\alpha_c - \alpha_a} \right| \left(\frac{dX_T}{d\gamma} \right) \quad (5.23)$$

Using this approach Kelly and Burchell (1994b) reconciled the apparent non-linear behaviour in the creep behaviour of H-451 graphite, confirming a linear relationship for creep strain against dose. See Fig 5.5.

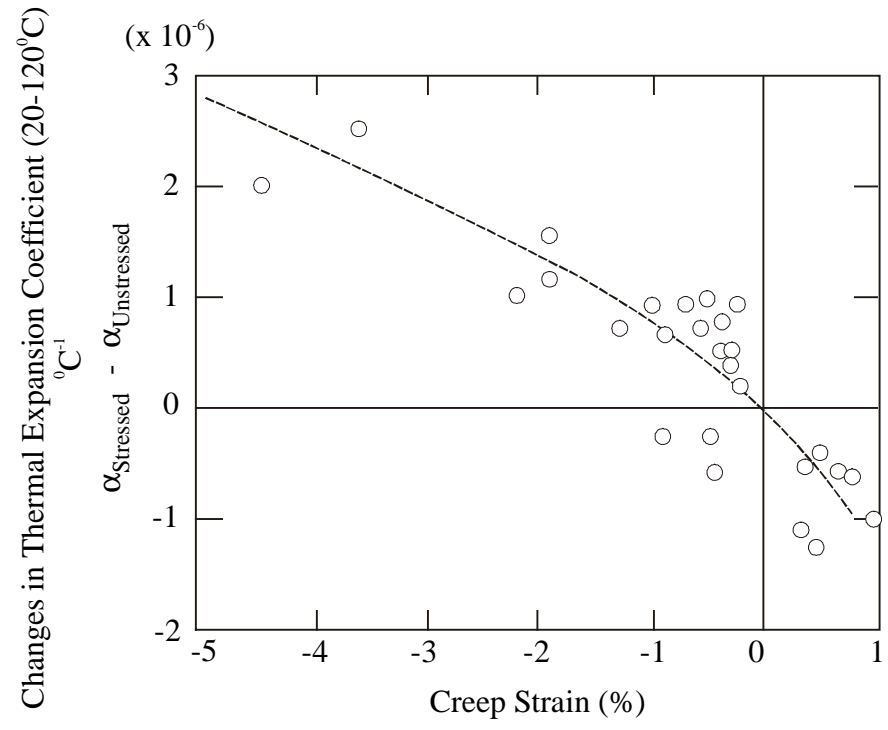


Figure 5.4 Effect of creep strains on thermal expansion coefficient measured parallel to stress axis for Gilsocarbon graphite

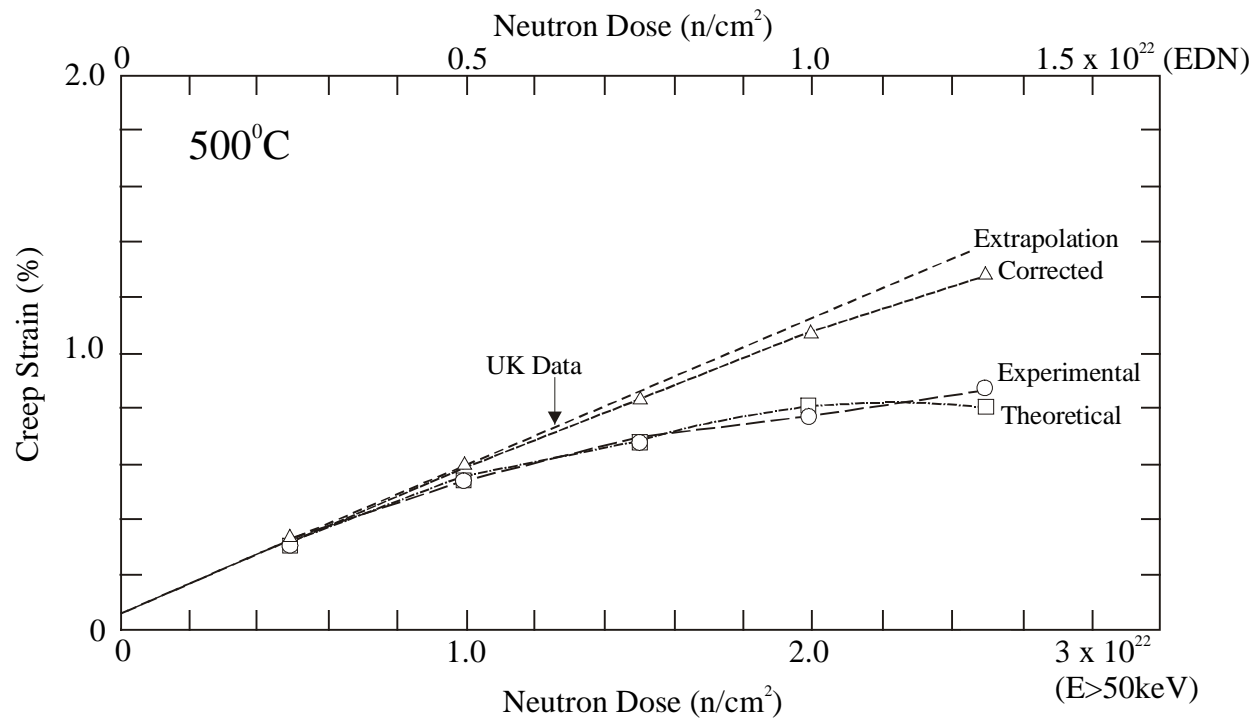


Figure 5.5 Comparison of experimental apparent creep strains at 500°C (HFR, PETTEN) against predicted apparent creep strains for 5MPa stress, and UK data

The implications of this to the reactor designer are most relevant in the multi-axial case where significant multi-axial strains can be generated. To enable these three-dimensional effects to be accounted for, information on the lateral changes in the thermal expansion coefficient as a function of creep strain were required. Unfortunately there is little reliable information on the transverse changes to the thermal expansion coefficient due to irradiation creep. However, there is now information on the change in thermal expansion coefficient which has been measured on stressed unirradiated Gilsocarbon graphite (Marsden *et al*, 1995, 1996).

This work revealed an unexpected result, changes to the thermal expansion coefficient due to compressive and tensile loading at relatively small elastic strains were of the same order as in the case of significant creep strains, see Fig 5.6.

The lateral coefficient gave a value of ~ 0.16 , the same order as the elastic Poisson's ratio, although subject to significant scatter.

The strength of graphite is well known to increase with irradiation, Brocklehurst (1977), to a point where the properties decline due to large structural effects. Up to this point the strength in tension and shear increases according to

$$\sigma_f(\gamma, T) \geq \sigma_0 \left| \frac{E}{E_0} \right|^{\frac{1}{2}} \quad (5.24)$$

where σ_0 is the unirradiated strength in the same direction and mode, and E and E_0 are the irradiated and unirradiated values of Young's modulus.

The relationship above can be arrived at from the Griffith-Orowan theory of fracture of materials containing cracks. This gives the condition for propagation of a crack:

$$\sigma_f \sim \left| \frac{E\gamma}{C} \right|^{\frac{1}{2}} \quad (5.25)$$

neglecting numerical constants, where γ is the effective surface energy per unit area, E is the elastic modulus and C is the crack length. If both C and γ can be considered to be independent of dose, the inequality in equation (5.24) could be replaced by the equality sign.

Early work by Losty and Orchard (1963) at low dose and low temperature where changes to the macrostructure due to micro-structural changes in the crystallite could be expected to be small showed that the elastic strain energy to failure σ^2/E remained essentially constant. This is consistent with the Griffith - Orowan theory for no change in C or γ .

Irradiation experiments at 150 °C by Taylor *et al* (1967) showed that after fast neutron irradiation the strain energy to failure increased at first with increasing dose and then decreased. He postulated that the increase was due to an increase in γ and the decrease was due to an increase in C . He explained the increase in γ as being due to the initial reduction in plasticity with dose and the increase in C as being due to crack generation at higher doses.

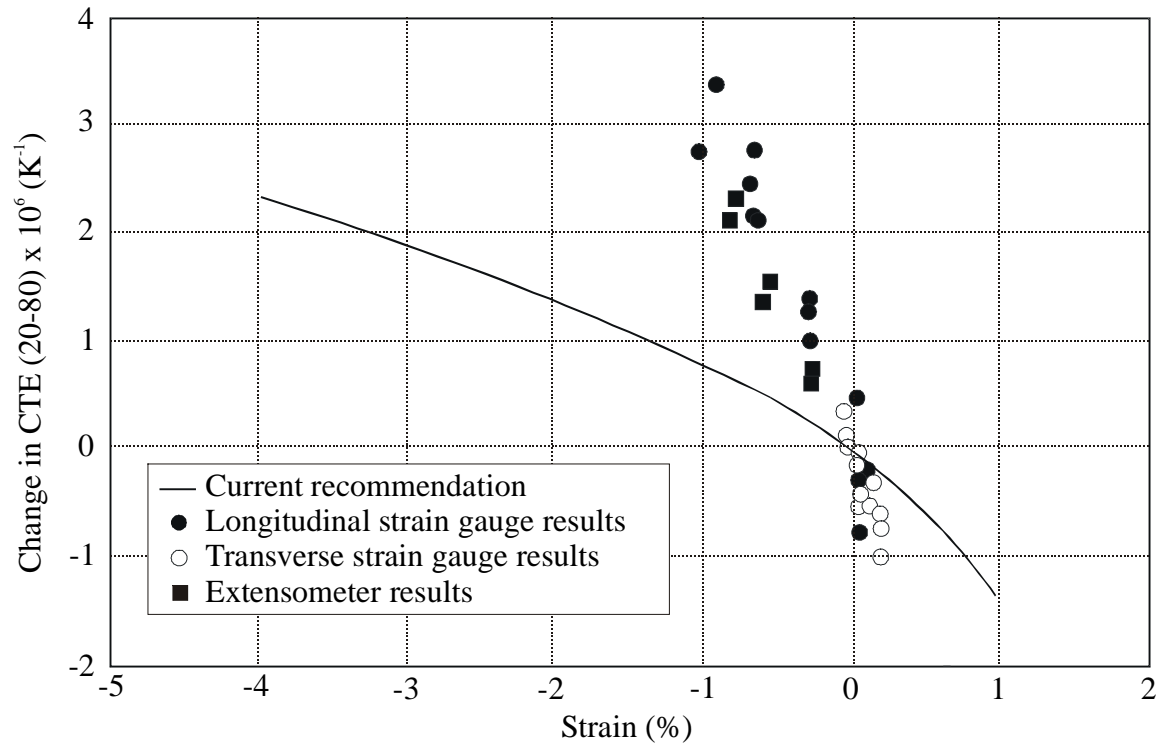


Figure 5.6 Change in thermal expansion coefficient versus strain for Gilsocarbon graphite

Gilsocarbon graphite irradiated at higher temperatures, 900-1200 °C, by Everett and Ridealgh (1972) showed an almost linear relationship between modulus and strength. This was similar to the findings of Engle (1977) who irradiated H-451 graphite in the range 600-1350 °C.

Fig 5.7 summarises the relationship between modulus and strength. At high temperatures, ~1000 °C, the strength-modulus relationship is at constant strain, whereas at lower temperatures the relationship is constant strain energy. At high irradiation doses and temperatures where structural effects are important the constant strain model appears to be more relevant.

Numerous attempts, Mason (1963), Amesz *et al* (1973) and Lungagnani and Krefeld (1972), have been made to fit statistical expressions to small sample data – particularly Weibull's. However, for practical reasons, the graphite samples tested are usually smaller than ~10 times the grain size. This leads to a problem when testing graphite. In the case of tensile loading, the strength increases with increasing specimen volume until it eventually becomes constant. However the strength of bend samples increase with specimen volume at first and pass through a maximum before decreasing and to obtain good Weibull parameters large samples are required.

In recent years attempts have been made to produce graphite failure models based on the graphite microstructure, the most developed of these being that by Tucker and co-workers (1986, 1993).

They looked at six commonly used graphite failure models, three simple models based on critical strain, critical stress and critical strain energy density, a statistical model due to Weibull, the so-called Rose/Tucker model, and a fracture mechanics approach; and reviewed the performance of these models against experimental data for a variety of tests in bend and tension.

Both critical stress and critical strain failure criteria do not take account of changes to the microstructure during loading and thus give poor correlations. Critical strain energy density depends on the volume of material being considered; this is ambiguous in its application.

Weibull statistical theory, previously discussed in relation to specimen size, is based on the failure strength of an i th elementary volume being described by the function

$$g(\sigma_i) = A_i m \sigma_i^{m-1} \exp(-A_i \sigma_i^m) \quad (5.26)$$

where σ_i is the stress on the i th volume dV_i , assumed to contain defects, m is the Weibull modulus and A_i is given by $A' dV_i$, where A' is a constant for a given material and type of loading. It is assumed that the probability of failure of an elemental volume under tensile stress will lead to catastrophic failure of the component.

The Rose/Tucker model is based on work by Buch (1976) and tries to take account of the microstructure of the graphite. The material is divided into small volumes typical of a particle size containing crystals of random orientation. The crystals are assumed to cleave only along the basal plane when the stress reaches a critical value. Under increasing load the probability of failure of each plane is calculated until a critical size is reached which satisfies the Griffith brittle failure criteria. Pores are treated as elemental volumes with no cleavage strength and the distribution of these is related to the microstructure porosity of the graphite under study.

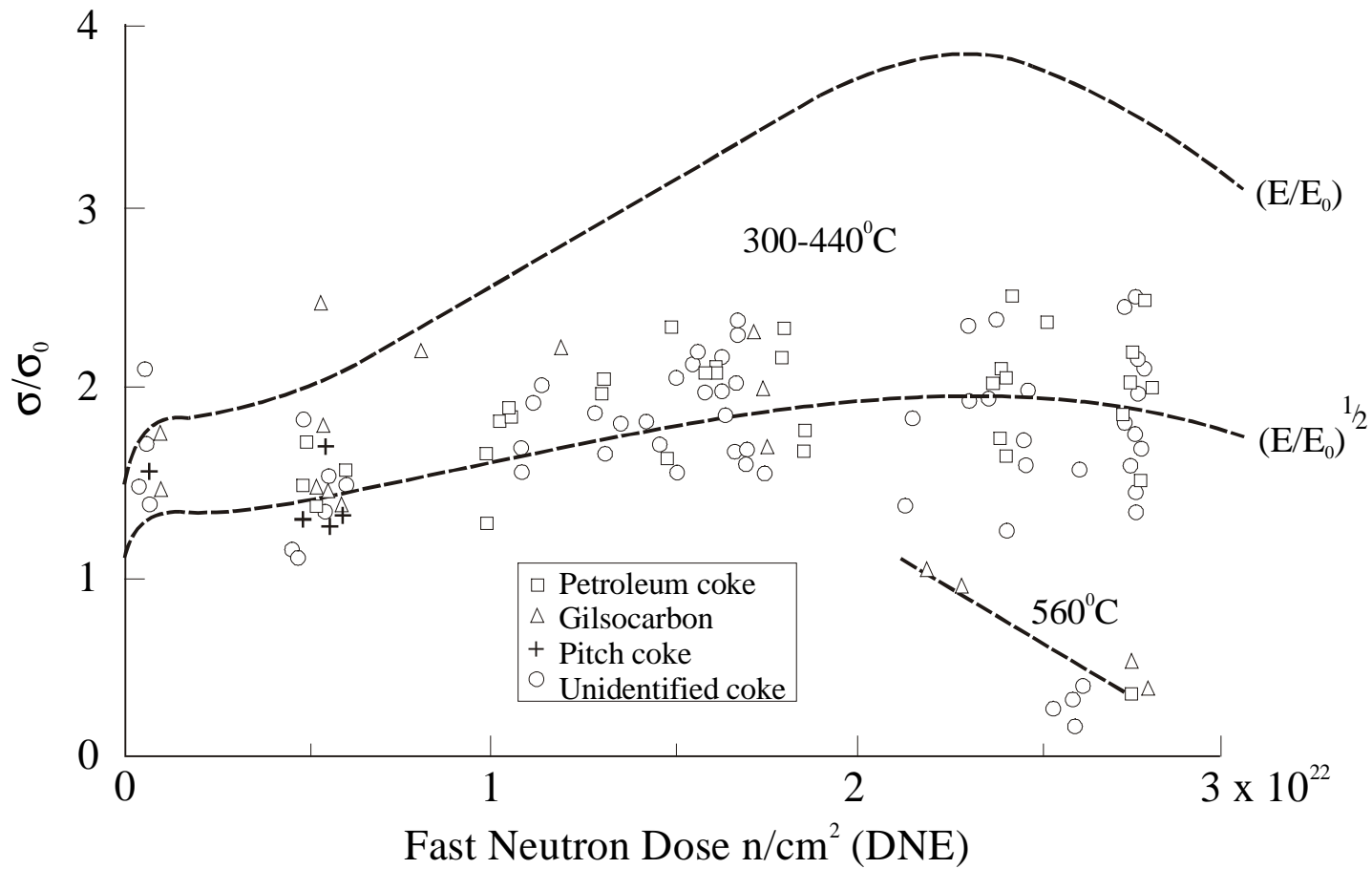


Figure 5.7 Tensile strength changes with fast neutron dose for near-isotropic graphites irradiated in DFR

In the fracture mechanics approach it is assumed that the graphite contains defects in the most damaging position in the model. The size of the defect is related to the structure of the graphite, but is otherwise insensitive to the microstructural changes, which give rise to failure.

The simple criteria based on critical strain, critical stress and strain energy density gave poor predictions for failure in most of the tests. The Weibull approach gave good correlation for geometry-related effects, but poor results for changes to microstructure. The Rose/Tucker and fracture mechanics approach gave the best results, which led to a further model, Tucker and McLachlan (1993), based on the last two approaches. More recent work by Burchell (1994) simplified and improved the Tucker and McLachlan model.

These graphite failure models have only been partially successful in describing failure in irradiated graphites and there is scope for further development in this area for practical application to reactor systems.

REFERENCES

- [1] Amelinckx S. and Delavignette P. *J. Applied Physics*, **31**, 2126 (1960).
- [2] Amelinckx S., Delavignette P. and Heerschap M. *Chemistry and Physics of Carbon*, **1** (Ed. P.L. Walker, Jr), Marcel Dekker, New York, 1 (1966).
- [3] Amesz J., Donea J. and Lanza F. *Extended Abstracts Eleventh Biennial Carbon Conf.* (USAEC Rep. Conf. 730601), 221 (1973).
- [4] Ayasse J.B. and Bonjour E. *Proc. Fourth SCI Conference on Industrial Carbons and Graphites*, SCI, London, 620 (1976).
- [5] Baker C. and Kelly A. *Phil. Mag.*, **9**, 927 (1964).
- [6] Birch M. PhD Thesis, University of Liverpool (UKAEA Report ND-R-590 (S/X)) (1981).
- [7] Brocklehurst J.E. *Chemistry and Physics of Carbon*, **13** (Eds. P.L. Walker, Jr and P.A. Throver), Marcel Decker, New York, 145 (UKAEA Report TRG 2731(S)) (1977).
- [8] Brocklehurst J.E. and Kelly B.T. *Carbon*, **31**, 155 (1993).
- [9] Buch J.D. *Properties Related to Fracture Toughness*, ASTM STP 605, 124 (1976).
- [10] Burchell T D, *Carbon* 1994
- [11] Chou Y.T. and Eshelby J.D. *J. Mech. Phys. Solids*, **10**, 27 (1962).
- [12] Davidson H.W. and Losty H.H.W. *Proc. Second International Conference on the Peaceful Uses of Atomic Energy*, United Nations, **7**, 307 (1958).
- [13] Eshelby J.D. *Phil. Mag.*, **40**, 903 (1949).
- [14] Engle G.B. *Assessment of Grade H-451 Graphite for Replaceable Fuel and Reflector Elements in HTGR*, US Report GA-A14690 (1977).
- [15] Everett M.R. and Ridealgh F. *Int. Conf. Carbon*, Baden-Baden (1972).
- [16] Friedel J. *Phil. Mag.*, **44**, 444 (1953).
- [17] Goggin P.R. and Reynolds W.N. *Phil. Mag.*, **16**, 317 (1967).
- [18] Gray W.J. *Carbon*, **11**, 383 (1973).
- [19] Jenkins G.M. and Jouquet G. *Carbon*, **6**, 85 (1968).
- [20] Kelly B.T. *Phil. Mag.*, **9**, 721 (1964).
- [21] Kelly B.T. and Foreman A.J.E. *Carbon*, **12**, 151 (1974).
- [22] Kelly B.T. and Brocklehurst J.E. *3rd Conf. Ind. Carbon and Graphite*, 363 (1972).
- [23] Kelly B.T. and Brocklehurst J.E. *J. Nuc. Mat.*, **65**, 79 (1977).
- [24] Kelly B.T. and Burchell T.D. *Carbon*, **32**, 499 (1994a).
- [25] Kelly B.T. and Burchell T.D. *Carbon*, **32**, 119 (1994b).
- [26] Kennedy C.R. USAEC Report ORNL-3951 (1966a).
- [27] Kennedy C.R. USAEC Report ORNL-4036 (1966b).
- [28] Kennedy C.R., Cook W.H. and Eatherly W.P. *Extended Abstracts from 13th Biennial Carbon Conference*, Irvine, 342 (1977).
- [29] Kennedy C.R. and Eatherly W.P. *Extended Abstracts from 14th Biennial Carbon Conference, Pennsylvania*, 453 (1979).
- [30] Kinchin G.H. *Proceedings of the United Nations Conference on the Peaceful Uses of Atomic Energy*, **7**, 472 (1956).
- [31] Losty H.H.W. *Proc. Fourth Biennial Carbon Conference*, Pergamon Press, New York, 593 (1960).
- [32] Losty H.H.W. *Uranium and Graphite*, Institute of Metals, Monograph No. 27, 81 (1962).
- [33] Losty H.H.W., Fielder N.C., Bell I.P. and Jenkins G.M. *Proc. Fifth Conference on Carbon*, Pergamon Press, **1**, 266 (1962).
- [34] Losty H.H.W. and Orchard J.S. *Proc. Fifth Biennial Carbon Conference*, **1**, Pergamon Press, New York, 519 (1963).

- [35] Lungagnani V. and Krefeld R. *Proc. Conf. On Continuum Aspects of Graphite Design*, Gatlinburg, 1970, USAEC Rep. Conf. 701105 (1972).
- [36] Markham M.F. *Materials Research*, 107, July (1962).
- [37] Marsden B.J., Preston S.D., Davies M.A. and McLachlan N. *Proc. Conf. Carbon 96*, Newcastle (1996).
- [38] Marsden B.J., Preston S.D., McLachlan N. and Davies M.A. *IAEA Conf. Graphite Moderator Lifecycle Technologies*, Bath, 24th-27th September (1995).
- [39] Mason I.B. *Proc. Fifth Biennial Carbon Conf.*, **2**, Pergamon Press, New York, 597 (1963).
- [40] Morgan W.C. *The Effect of Low Compressive Stresses on Radiation-Induced Dimensional Changes in Graphite*, GE Report HW-SA-2925 (1963).
- [41] Mott N.F. *Phil. Mag.*, **43**, 1151 (1952).
- [42] Perks A.J. and Simmons J.H.W. *Carbon*, **1**, 441 (1964).
- [43] Platonov P.A. *Proc. Int. Conf. Irradiation Damage in Reactor Materials*, **1**, IAEA, Vienna, 417 (1969).
- [44] Seldin E.J. and Nezbeda C.W. *J. Applied Physics*, **41**, 3389 (1970).
- [45] Simmons J.H.W. *Proc. Third Biennial Conference on Carbon*, Pergamon Press, New York, 559 (1957).
- [46] Simmons J.H.W. *Radiation Damage in Graphite*, Pergamon Press (1965).
- [47] Summers L., Walker D.C.B. and Kelly B.T. *Phil. Mag.*, **14**, 317 (1966).
- [48] Taylor R., Brown R.G., Gilchrist K., Hall E., Hodds A.T., Kelly B.T. and Morris F. *Carbon*, **5**, 519 (1967).
- [49] Tucker M.O., Rose A.P.G. and Burchell T.D. *Carbon*, **24**, 581 (1986).
- [50] Tucker M.O. and McLachlan N. *J. Physics D: Appl. Phys.*, **26**, 893 (1993).
- [51] Woolley R.L. *Phil. Mag.*, **11**, 179 (1965).

